

$$\ln s = 0.50 N - 2.8 \quad (7)$$

where N is expressed in revolutions per second. Using this relation and Eq. 6 one obtains the calculated k_L values in column 7 of Table 1, in somewhat better agreement with the experimental data in column 8.

Our conclusions are as follows:

- (i) The surface region of the stirred cell is turbulent.
- (ii) The distribution of the large (integral scale) eddies near the surface agrees well with the Danckwerts distribution function (Eq. 5), though there is a tendency for the larger eddies to be replaced more slowly than this equation predicts.
- (iii) The eddies responsible for most of the mass transfer are larger and of lower frequency than the integral scale or Prandtl eddies, i.e., the small x -directional movements in the surface are less important in mass transfer than are the larger movements which relate to "surface renewal."

NOTATION

D	= molecular diffusivity, $\text{m}^2\cdot\text{s}^{-1}$
f	= frequency of eddies, s^{-1}
k_L	= mass transfer coefficient on liquid side of surface $\text{m}\cdot\text{s}^{-1}$
l	= eddy length, mm
l_L	= macroscale of eddies, mm
L	= tip-to-tip length of stirrer blade, mm
N	= shaft speed, revolutions per second
$Q(\Delta t)$	= velocity autocorrelation coefficient with respect to time $\text{m}^2\cdot\text{s}^{-2}$
$Q^*(\Delta t)$	= $Q(\Delta t)/(v'_x)^2$, dimensionless

Re	= Reynolds number ($= NL^2/\nu$), dimensionless
s	= frequency of surface renewal, s^{-1}
t	= time, s or ms
t_L	= eddy macro-timescale, s
\bar{v}_x	= mean overall velocity of flow in the x -direction (along the surface), $\text{m}\cdot\text{s}^{-1}$
v'_x	= fluctuation velocity, $\text{m}\cdot\text{s}^{-1}$
\bar{v}'_x	= root mean square value of v'_x , $\text{m}\cdot\text{s}^{-1}$
ν	= kinematic viscosity, m^2s^{-1}
ϕ	= surface age distribution function of Danckwerts theory, s^{-1}

LITERATURE CITED

- Danckwerts, P. V., "Significance of Liquid-Film Coefficients in Gas Absorption," *Ind. Eng. Chem.*, **43**, p. 1460 (1951).
- Davies, J. T., *Turbulence Phenomena*, Academic Press, New York (1972).
- Davies, J. T., "Interfacial Effects in Gas Transfer to Liquids," *Chem. and Ind.*, p. 189 (1980).
- Davies, J. T., and W. Khan, "Surface Clearing by Eddies," *Chem. Eng. Soc.*, **20**, p. 713 (1965).
- Davies, J. T., and F. J. Lozano, "Turbulence Characteristics and Mass Transfer at Air-Water Surfaces," *AICHE J.*, **25**, p. 405 (1979).
- Higbie, R., "The Rate of Absorption of a Pure Gas into a Still Liquid During Short Periods of Exposure," *Trans. AICHE*, **31**, p. 365 (1935).
- Springer, T. G., and R. L. Pigford, "Influence of Surface Turbulence and Surfactants on Gas Transport Through Liquid Interfaces," *Ind. Eng. Chem. Fund.*, **9**, p. 458 (1970).

Manuscript received January 4, 1982; revision received June 24, and accepted July 20, 1982.

Observations on Catalytic Dissociation of Ammonia at High Temperatures and Pressures

SUBHASHIS NANDY

and T. G. LENZ

Department of Agricultural and Chemical Engineering
Colorado State University
Fort Collins, CO 80523

INTRODUCTION

There has been relatively little work done on ammonia dissociation under high temperature and pressure conditions. Conventional promoted iron catalyst used effectively for synthesis of ammonia cannot be used for the dissociation reaction at high pressures since at temperatures greater than 550°C this catalyst sinters. Hence, we undertook a study of this dissociation reaction, at substantial pressures using other catalyst materials.

EXPERIMENTAL

Our experimental studies were performed in a plug flow reactor, where the pressure was maintained between 6.9 and 10 MPa (68 and 100 atm), the temperature between 875 and 1,050 K, the ammonia flow rate between 0.12 and 0.60 kg/h and the weight of the catalyst between 0.006 and 0.01 kg.

A schematic diagram of the experimental apparatus is shown in Figure 1. A detailed description of this apparatus is given elsewhere (Nandy et al., 1981). Basically, the system comprises a plug flow reactor, which is heated electrically. Ammonia is pumped into the reactor and the degree of dissociation is measured from the flow rate of exiting nitrogen and hydrogen.

The dissociation reaction conditions are similar to the reaction conditions

S. Nandy is presently at the Department of Chemical Engineering, Pennsylvania State University, University Park, PA 16802.

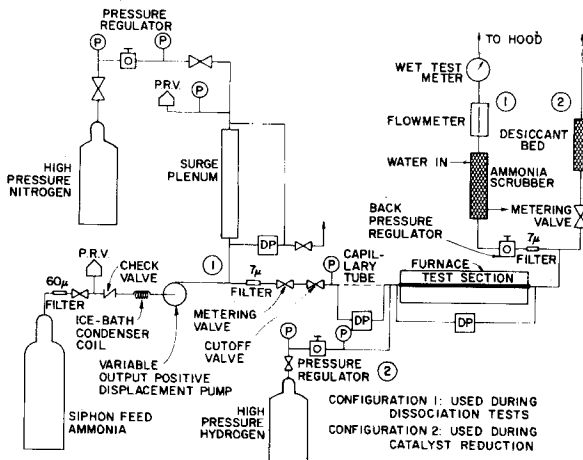


Figure 1. Schematic of single-tube reactor experimental loop.

TABLE 1. CATALYST PROPERTIES

Catalyst	Avg. Size, m	Surface, m ² /kg	Bulk Density, kg/m ³	Crushing Strength, kg
6.9 wt. % Ni on α -Al ₂ O ₃	0.002	4×10^3	1.28×10^3	36.3
8.1 wt. % Ni on γ -Al ₂ O ₃	0.001	8×10^5	1×10^{-3}	27.2

from steam reforming of methane. A catalyst often used for the latter purpose is nickel metal supported on alumina (Satterfield, 1980). Since ammonia dissociation reaction conditions are similar to those for steam reforming, it seemed reasonable to assume that a similar catalyst would perform equally well for the ammonia reaction.

The catalyst materials used for our ammonia dissociation studies were prepared by United Catalysts, Inc. of Louisville, Kentucky. The above table summarizes the physical properties of these catalysts.

As received, the catalyst materials were in the oxide state, and had to be reduced before dissociation tests were run. For catalyst reduction, loop configuration 2 (Figure 1) was used. In this configuration, nitrogen or hydrogen gas was inlet to the test section [generally at about 0.56 MPa (5-4 atm)]. The gas from the test section passed through a metering valve and then through a desiccant bed. Careful monitoring of the desiccant material weight gain enabled assessing the amount of water produced during the catalyst reduction process. The reduction procedure consisted of first passing nitrogen gas through the reactor at 675 K to drive off any adsorbed water. According to Nielsen (1968), the effect of pressure on reduction is not important. After elimination of adsorbed water, hydrogen was passed through the reactor to reduce the nickel oxide to metallic nickel, using a hydrogen flow rate of 9×10^{-5} m³/min. The reduction process was continued until there was no significant water evolved.

TRANSPORT EFFECTS

The overall rate for ammonia dissociation may be affected by:

1. Gas-phase mass transfer of the gaseous reactant or products to or from the catalyst surface.
2. Heat transfer from the bulk fluid to the catalyst surface.
3. Mass and heat transfer within the catalyst pellet pore structure.
4. Intrinsic surface reactions.

The heat and mass transfer resistances of the film surrounding the catalyst particle were calculated using the conventional J-factor approach (Yang and Hougen, 1950). These calculations indicated that heat and mass transfer resistances of the film were negligible for the observed reaction rates. The intraparticle mass transfer limitation was calculated using the correlation developed by

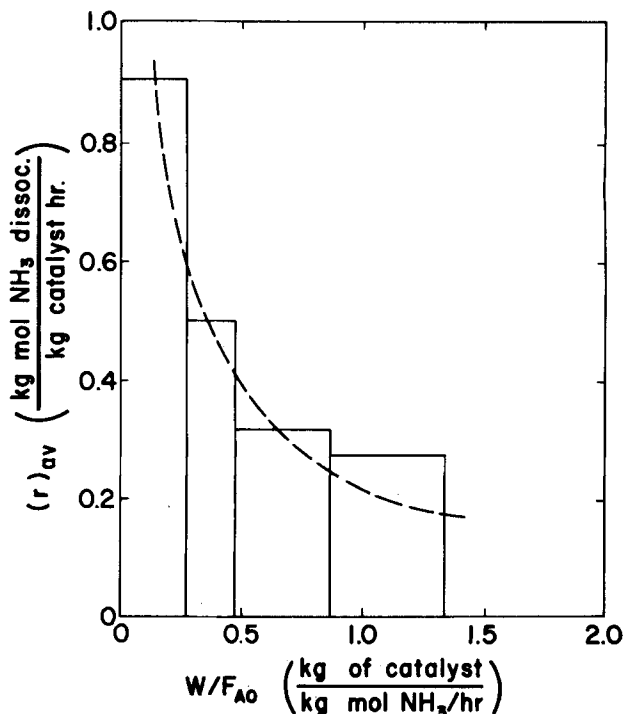


Figure 2. Average rate of NH₃ dissociation for Ni-catalyst at 1,025 K and 10 MPa.

Hudgins (1968). It was found that concentration gradients through the pellet were not significant. The absence of temperature gradients in the catalyst particle was also established using the correlation of Anderson (1963). Actual measurements during experiments indicated a maximum ΔT of 10 K across the catalyst bed (for a maximum dissociation of 60%).

The rate of dissociation of ammonia, r_A (kmol NH₃ dissociated/kg catalyst · h) is given by the following expression:

$$r_A = dX_A/d(W/F_{AO}) \quad (1)$$

Equation 1 implies a plug flow assumption, and we employed the criterion of Mears (1971) to demonstrate that axial dispersion effects along the reactor length were minimal for our experiments, and that we could thus use Eq. 1 for data analysis.

RESULTS

The above transport calculations indicated that reaction on the surface of the catalyst should be rate limiting (Nandy et al., 1981; Nandy, 1981). Temkin and Pyzhev (1940) proposed that the rate-limiting step in the synthesis and decomposition of ammonia on the surface of a heterogeneous catalyst is the adsorption and desorption of nitrogen and that nitrogen atoms are the main adsorbed species on the catalyst surface. They also proposed that the activation energies for adsorption and desorption on the catalyst surface vary linearly with coverage. The rate expression that they proposed is:

$$r_A = k[(NH_3)^2/(H_2)^3]^{0.5} \quad (2)$$

$$\text{or, } r_A = ky_{NH_3}y_{H_2}^{-1.5}P^{-0.5} \quad (3)$$

The rate constant k is obtained from Eq. 3 and may be expressed as:

$$k = r_A/[b] \quad (4)$$

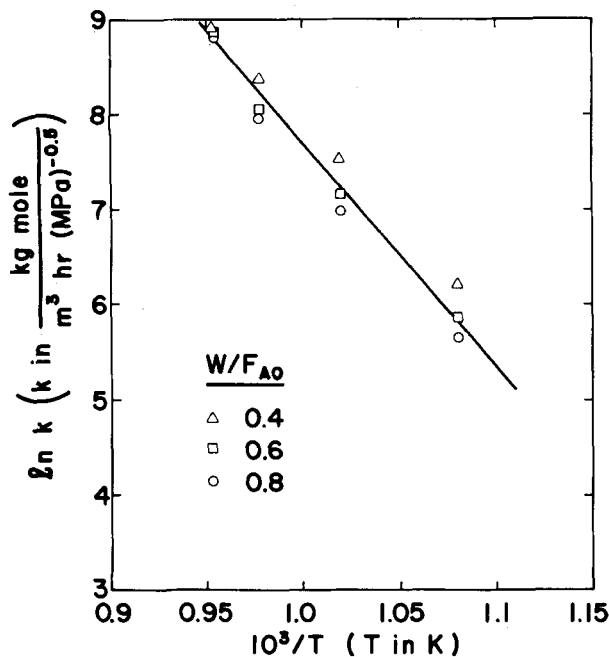


Figure 3. Representative Arrhenius plot.

where the term b contains y 's and P .

We estimated r_A as a function of W/F_{AO} by drawing an equal area curve through a plot of $\Delta X_A / \Delta(W/F_{AO})$ vs. W/F_{AO} . One such curve is shown in Figure 2. This method of analysis is that suggested by Churchill (1974) as superior to drawing tangents.

For each catalyst material, for three different values of W/F_{AO} , Arrhenius activation energy (E_A) and preexponential factor (k_0) values were determined in the following way. For the first value of W/F_{AO} , a plot of W/F_{AO} vs. r_A at one particular temperature gives r_A . Then, we use a plot of W/F_{AO} vs. X_A at the same temperature to estimate X_A , thus obtaining y_{NH_3} and y_{H_2} . The values of r_A , y_{NH_3} and y_{H_2} then give k from Eq. 3 or 4. This procedure is repeated for at least three different temperatures for the same value of W/F_{AO} . An Arrhenius plot such as that shown in Figure 3 is then utilized to obtain the slope and intercept of the best straight line fit between $\ln k$ and $1/T$. The slope gives E_A/R , from which E_A is readily calculated, while k_0 is calculated from the intercept. This procedure is repeated for two other values of W/F_{AO} . Table 2 shows one set of representative data collected during our studies. The results of our studies are summarized in Table 3.

CONCLUSIONS

The principal conclusions drawn from our dissociation experiments are:

1. For ammonia dissociation with nickel catalyst (on α - and γ -alumina substrates) at high pressure, the resistances offered by the gas film surrounding the catalyst pellets are not of primary importance. More specifically, we have found that the concentration and temperature gradients across this film are negligible. In addition, intraparticle temperature and ammonia concentration gradients are also negligible for dissociation over nickel catalyst at pressures of 6.9–10 MPa and temperatures of 875–1,050 K.

2. For the nickel catalyst on α -alumina (6.9 wt.% Ni), the activation energy value varied between 258×10^3 kJ/kg mol (61.7 kcal/mol) and 283×10^3 kJ/kg mol (67.6 kcal/mol). However, for the nickel catalyst on γ -alumina (8.1 wt.% Ni) the activation energy was found to be about 190×10^3 kJ/mol (45.4 kcal/mol).

The difference between the two activation energy values for the two different catalyst materials may be partially attributed to the difference in their surface areas and effective reduction of each

TABLE 2. KINETIC MEASUREMENTS WITH 6.9 WT. % NI (ON α -ALUMINA SUBSTRATE) CATALYST AT 9.9 MPa (98 atm)

Temp. K	W/F_{AO} kg/kmol/h	% Ammonia Dissoc.
875	0.478	5.9
925	0.465	12.3
975	0.411	23.0
1,025	0.478	35.3
875	0.822	7.2
925	0.682	12.4
975	0.582	24.3
1,025	0.859	48.7
875	1.779	8.9
925	1.524	15.6
975	1.016	37.8
1,025	1.338	61.7

TABLE 3. ACTIVATION ENERGY FOR NICKEL CATALYST

Catalyst	Pressure	W/F_{AO} kg Catalyst kmol/h	E_A kJ kmol	k_0 m ³ ·h·(Pa) ^{-0.5}
6.9 wt. % Ni on α -Alumina	6.9 MPa	0.6–0.8	274×10^3	4.0×10^{27}
6.9 wt. % Ni on α -Alumina	9.8 MPa	0.6–0.8	258×10^3	1.3×10^{26}
8.1 wt. % Ni on γ -Alumina	6.9 MPa	0.6–0.8	192×10^3	1.6×10^{22}

catalyst. The surface area that is measured may not, however, be the area effective for catalysis. Only certain parts of the surface, the active centers, are active for chemisorption of a reactant. It might have been possible that for the γ -alumina support, the metallic nickel were dispersed fairly well on the catalyst surface, which provided more active centers for the dissociation reaction. However, in the case of α -alumina support, the nickel metal might not have been dispersed properly and the dissociation reaction proceeded more slowly than on γ -alumina (thus giving higher activation energy values). The decrease in preexponential factor values with decrease in activation energy values may be due to an energetically heterogeneous surface. It might be possible that different active sites have different catalytic properties, with more highly active sites making it much easier for the dissociation reaction to take place. The activation energy value obtained in the current experiment for α -alumina substrate is in reasonable agreement with the available literature values of 160 – 168×10^3 kJ/kmol (38.2–40.2 kcal/mol) (Loffler, 1976; Nielsen, 1968).

3. The effect of pressure on the activation energy value for the same catalyst is small. This is evident from the data obtained for nickel catalyst on α -alumina at two different pressures, where the difference between 274×10^3 kJ/kmol (65.5 kcal/mol) and 258×10^3 kJ/mol (61.7 kcal/mol) likely results from other factors than pressure, such as catalyst batch and reduction.

ACKNOWLEDGMENT

The authors are grateful for the financial support of this research through a DOE/SERI contract. We would also like to acknowledge J. A. Harris and J. H. Wright for their assistance in this research.

NOTATION

b	$= y_{NH_3} y_{H_2}^{-1.5} p^{-0.5}$
E_A	= activation energy, kJ/kmol

F_{AO}	= input flow rate of ammonia kmol/h
(i)	= surface concentration of i th component
k	= rate constant for dissociation reaction, kmol/m ³ ·h·(Pa) ^{-0.5}
k_0	= preexponential factor, k mol/m ³ ·h·(Pa) ^{-0.5}
P	= total pressure, Pa
r_A	= rate of reaction, kmol ammonia dissociated/h·kg catalyst
R	= gas constant, kJ/kmol·K
T	= temperature of reaction, K
W	= weight of catalyst, kg
X_A	= kmol ammonia dissociated/kmol ammonia feed
y_i	= mole fraction of component i

LITERATURE CITED

Anderson, J. B., "A Criterion for Isothermal Behavior of a Catalyst," *Pellet. Chem. Eng. Sci.*, **18**, p. 147 (1963).
 Hudgins, R. R., "A General Criterion for Absence of Diffusion Control in an Isothermal Catalyst Pellet," *Chem. Eng. Sci.*, **23**, p. 94 (1968).
 Churchill, S. W., *The Interpretation and Use of Rate Data*, Hemisphere Publishing Corp. (1979).
 Loffler, D. G., "Ammonia Decomposition on Platinum and Iron: An Ap-

plication of Langmuir-Hinshelwood Rate Expressions," Ph.D. Dissertation, University of Minnesota, Minneapolis (1976).
 Mears, D. E., "Tests for Transport Limitations in Experimental Catalytic Reactors," *Ind. Eng. Chem. Process Design and Develop.*, **10**, p. 541 (1971).
 Nandy, S., T. G. Lenz, J. A. Harris, and J. H. Wright, "Evaluation of Candidate Catalysts for an Ammonia-Based Solar Thermochemical Receiver," *Proc. 1981 Amer. Soc. of Int. Solar Energy Soc. Annual Meeting*, Philadelphia, p. 437 (1981).
 Nandy, S., "Observations on Catalytic Dissociation of Ammonia at High Pressures," M.S. Thesis, Colorado State University, Fort Collins (1981).
 Nielsen, A., *An Investigation on Promoted Iron Catalysts for the Synthesis of Ammonia*, 3rd Ed., Gjellerup, Copenhagen (1968).
 Ozaki, A., H. S. Taylor, and M. Boudart, "Kinetics and Mechanism of the Ammonia Synthesis," *Proc., Roy. Soc., London*, **A258**, p. 47 (1960).
 Satterfield, C. N., *Heterogeneous Catalysis in Practice*, McGraw-Hill, New York (1980).
 Temkin, M., and V. Pyzhev, "Kinetics of the Synthesis of Ammonia on Promoted Iron Catalysts," *Acta Physicochimica, U.R.S.S.*, **12**(3), p. 327 (1940).
 Yang, K. H., and O. A. Hougen, "Determination of the Mechanism of Catalyzed Gaseous Reactions," *Chem. Eng. Prog.*, **46**(3), p. 146 (1950).

Manuscript received January 18, 1982; revision received November 18, and accepted December 14, 1982.

A Lagrangian Finite Element Method for the Simulation of Flow of Newtonian Liquids

P. BACH and O. HASSAGER

Institutet for Kemiteknik
 Danmarks Tekniske Højskole
 DK-2800 Lyngby, Denmark

INTRODUCTION

In the Lagrangian description, the fluid mechanical equations are formulated as an initial value problem. Thus, at an initial instant the location and velocity of all fluid particles are considered known, and the subsequent motion of the particles is then followed. An advantage of this description is that the transient motion of a free surface is described in a particularly simple fashion. Another possible advantage is that the nonlinear convective terms are absent, which means that it is simple to construct a stable implicit forward integration method.

The method described here is related to that of Hirt, Cook and Butler (1970) who used a Lagrangian method to solve the Navier Stokes equations. These authors, however, used a finite difference method; as a result their method for the application of boundary conditions is somewhat complicated. By contrast the finite element method enables a particularly simple application of the boundary conditions, both no-slip and slip conditions as well as free surface conditions. Thus Frederiksen and Watts (1981) have formulated a finite-element method for time-dependent incompressible flow, but these authors use the Eulerian formulation of the Navier Stokes equations. In the following it will be demonstrated how a simple Lagrangian finite element method may be implemented for an incompressible Newtonian liquid.

FLUID MECHANICAL EQUATIONS

At an initial time, t_0 , the space coordinates of all fluid particles to be considered are denoted x_i^0 ($i = 1, 2, 3$). The set of numbers (x^0, t_0) therefore denotes a particular fluid particle. Now for each fluid particle (x^0, t_0) , we wish to solve for the space coordinates $x_i = x_i(x^0, t_0, t)$, the Lagrangian velocity field $u_i = u_i(x^0, t_0, t)$ and the pressure field $p = p(x^0, t_0, t)$ as a function of time t for $t \geq t_0$. These variables are determined from the solution of the following initial value problem:

$$\frac{\partial}{\partial t} x_i(x^0, t_0, t) = u_i \quad (i = 1, 2, 3) \quad (1)$$

$$\rho \frac{\partial}{\partial t} u_i(x^0, t_0, t) = -\frac{\partial}{\partial x_i} p + \mu \sum_{m=1}^3 \frac{\partial^2}{\partial x_m \partial x_m} u_i + \rho g_i \quad (i = 1, 2, 3) \quad (2)$$

$$0 = \sum_{m=1}^3 \frac{\partial}{\partial x_m} u_m \quad (3)$$

with

$$(x_i, u_i) = (x_i^0, u_i^0) \text{ at } t = t_0 \quad (4)$$